

Roles of Surface Protonation on the Photodynamic, Catalytic, and Other Properties of Polyoxometalates Probed by the Photochemical Functionalization of Alkanes. Implications for Irradiated Semiconductor Metal Oxides

Roman F. Renneke, Miryam Kadkhodayan, Marzia Pasquali, and Craig L. Hill*

Contribution from the Department of Chemistry, Emory University, Atlanta, Georgia 30322.
Received November 21, 1990. Revised Manuscript Received June 24, 1991

Abstract: This paper further addresses the photodynamic and redox properties of polyoxometalates and the legitimacy of these compounds as discrete molecular representations for semiconductor metal oxides. The effect of protonation on redox, photochemical, catalytic, and other basic properties of a representative polyoxometalate, decatungstate ($W_{10}O_{32}^{4-}$), in aprotic media has been examined in detail. Protonation results in minimal perturbation of the electronic absorption spectral features of $W_{10}O_{32}^{4-}$ including the HOMO-LUMO gap (band gap in semiconductor formalism) but a shift of ~ 1 V in the ground-state redox potentials (two quasi-reversible one-electron waves at -1.2 and -1.8 V become one quasi-reversible two-electron wave at -0.1 V vs $Ag/AgNO_3$). The quantum yields (Φ) for the photooxidation of several alkanes by $W_{10}O_{32}^{4-}$ (homogeneous reactions in CH_3CN solution, $25^\circ C$, Ar atmosphere, 322-nm light) all increase substantially upon protonation, with the increases dependent on alkane ($\Phi_{H^+}/\Phi_{noH^+} \approx 6.9$ for cyclooctane (least increase) to ~ 25 for most alkanes). The alkane oxidation products in these processes also change upon protonation from those largely derived from freely diffusing alkyl radical intermediates to those largely derived from carbocation intermediates. The EPR spectra (X band) obtained from photooxidation of alkanes by $W_{10}O_{32}^{4-}$ in the absence and presence of acid in frozen CH_3CN glasses at 10 K and at $25^\circ C$ along with evidence from UV-visible spectra and oxidative titration data establish that the one-electron (EPR-active, $S = 1/2$) and two-electron (EPR-silent, $S = 0$) reduced forms of decatungstate, $W_{10}O_{32}^{5-}$ and $W_{10}O_{32}^{6-}$, respectively, are produced in a 3:7 mol ratio in the absence of acid while the two-electron reduced form is produced exclusively in the presence of acid. EPR spectra as a function of irradiation time and as a function of acid concentration further establish that the two forms of the one-electron-reduced decatungstate present under acidic conditions are $W_{10}O_{32}^{5-}$ and $HW_{10}O_{32}^{4-}$. The quantum yields, organic product distributions, polyoxometalate product distributions, UV-vis spectra, and ground-state redox potentials have all been assessed as a function of the number of equivalents of acid added per equivalent of $W_{10}O_{32}^{4-}$. All change monotonically with added acid, are well correlated, and attain a limiting behavior when ~ 2.5 equiv of acid has been added. The addition of $W_{10}O_{32}^{4-}$ to acidified CH_3CN solutions of branched alkenes suppresses acid-catalyzed alkene isomerization, providing another independent confirmation of $W_{10}O_{32}^{4-}$ protonation. Protonation significantly decreases the rate of reduced decatungstate reoxidation by dioxygen in line with the effect of protonation on the ground-state redox potentials. The rate laws of the protonated and unprotonated forms are very similar: Both are variable order in $W_{10}O_{32}^{4-}$, apparently first order in substrate, and first order in light intensity. A rate law consistent with all the data that covers both protonation phenomena and the important coupled thermal process of electron-transfer oxidation of intermediate radicals has been formulated. The ratios of the rate constant for total deactivation of the excited state to the specific rate constant for alkane photooxidation by the excited state, assessed by double reciprocal plots, are 0.86 and 3.4 for the acidified and nonacidified reactions, respectively. The ratios of the rate constant for radiationless decay to that specifically for alkane photooxidation are 0.095 and 1.63 for the acidified and nonacidified systems, respectively.

Introduction

Early-transition-metal polyoxometalates and many semiconductor metal oxides, including TiO_2 , have a number of features in common. Both classes of materials are constituted by d^0 transition-metal and oxide ions, exhibit similar electronic attributes including well-defined HOMO-LUMO gaps (semiconductor "band gaps"), excited states with potent redox capabilities, and in some cases, similar structural elements.¹⁻⁵ As a consequence,

some polyoxometalates in some respects are experimentally tractable soluble molecular analogues of some semiconductor metal oxides.³ While there are a number of parallels between polyoxometalates and semiconductor metal oxides, there are also differences. One area of difference and one that has been exploited

(1) The following are reviews on early transition metal polyoxometalates. General reviews: (a) Pope, M. T. *Heteropoly and Isopoly Oxometalates*; Springer-Verlag: New York, 1983. (b) Day, V. W.; Klemperer, W. G. *Science* **1985**, *228*, 533. (c) Pope, M. T.; Müller, A. *Angew. Chem., Int. Ed. Engl.* **1991**, *30*, 34. Polyoxometalate nomenclature: (d) Jeannin, Y.; Fournier, M. *Pure Appl. Chem.* **1987**, *59*, 1529. Polyoxometalates in catalysis: (e) Misono, M. *Catal. Rev.-Sci. Eng.* **1987**, *29*, 269. (f) Kozhevnikov, I. V.; Matveev, K. I. *Russ. Chem. Rev. (Engl. Transl.)* **1982**, *51*, 1075. (g) Kozhevnikov, I. V.; Matveev, K. I. *Appl. Catal.* **1983**, *5*, 135. (h) Hill, C. L. In *Metal Catalysis in Hydrogen Peroxide Oxidations*; Strukul, G., Ed.; Reidel: Dordrecht, The Netherlands, 1991; Chapter 8, in press.

(2) Recent reviews of semiconductor metal oxide mediated photochemical oxidations or transformations of organic substrates: (a) Fox, M. A. *Acc. Chem. Res.* **1983**, *16*, 314. (b) *Homogeneous and Heterogeneous Photocatalysis*; Pelizzetti, E., Serpone, N., Eds.; NATO ASI Series C, Vol. 174; Reidel: Dordrecht, The Netherlands, 1986. (c) Pichat, P.; Fox, M. A. In *Photoinduced Electron Transfer*; Elsevier: Amsterdam, The Netherlands, 1988; Vol. D, pp 241-303. (d) Grätzel, M. *Heterogeneous Photochemical Electron Transfer*; CRC Press: Boca Raton, FL, 1989; Chapter 3. (e) *Photochemical Energy Conversion*; Norris, J. R., Jr., Meisel, D., Eds.; Elsevier: New York, 1989; Part IV and references cited in each.

(3) Direct parallels have been made between semiconductor metal oxides and polyoxometalates in the photooxidation of alcohols in the presence of O_2 : Fox, M. A.; Cardona, R.; Gaillard, E. *J. Am. Chem. Soc.* **1987**, *109*, 6347. The photoredox activity of semiconductor metal oxides and polyoxometalates under aerobic and anaerobic conditions have been contrasted: Chambers, R. C.; Hill, C. L. *Inorg. Chem.* **1991**, *30*, 2776.

(4) Recent representative papers on the photooxidation of organic substrates other than alkanes by polyoxometalates: (a) Akid, R.; Darwent, J. R. *J. Chem. Soc., Dalton Trans.* **1985**, 395. (b) Attanasio, D.; Suber, L. *Inorg. Chem.* **1989**, *28*, 3781. (c) Hill, C. L.; Bouchard, D. A. *J. Am. Chem. Soc.* **1985**, *107*, 5148. (d) Chambers, R. C.; Hill, C. L. *Ibid.* **1990**, *112*, 8427. (e) Nomiya, K.; Miyazaki, T.; Maeda, K.; Miwa, M. *Inorg. Chim. Acta* **1987**, *127*, 65. (f) Papaconstantinou, E. *Chem. Soc. Rev.* **1989**, *18*, 1. (g) Savinov, E. N.; Saidkhanov, S. S.; Parmon, V. N.; Zamaraev, K. I. *Dokl. Phys. Chem. (Engl. Transl.)* **1983**, *272*, 741. (h) Shul'pin, G. B.; Kats, M. M. *Zh. Obshch. Khim.* **1989**, *59*, 2738. (i) Ward, M. D.; Brazdil, J. F.; Mehandu, S. P.; Anderson, A. B. *J. Phys. Chem.* **1987**, *91*, 6515. (j) Yamase, T.; Watanabe, R. *J. Chem. Soc., Dalton Trans.* **1986**, 1669. (k) Yamase, T.; Suga, M. *J. Chem. Soc., Dalton Trans.* **1989**, 661.

(5) (a) Renneke, R. F.; Hill, C. L. *J. Am. Chem. Soc.* **1988**, *110*, 5461. (b) Chambers, R. C.; Hill, C. L. *Inorg. Chem.* **1989**, *28*, 2509. (c) Renneke, R. F. Ph.D. Thesis, Emory University, 1989. (d) Shul'pin, G. B.; Kats, M. M. *Bull. Acad. Sci. USSR, Div. Chem. Sci. (Engl. Transl.)* **1989**, *38*, 2202. (e) Prosser-McCartha, C. M.; Hill, C. L. *J. Am. Chem. Soc.* **1990**, *112*, 3671. (f) Renneke, R. F.; Pasquali, M.; Hill, C. L. *Ibid.* **1990**, *112*, 6585.

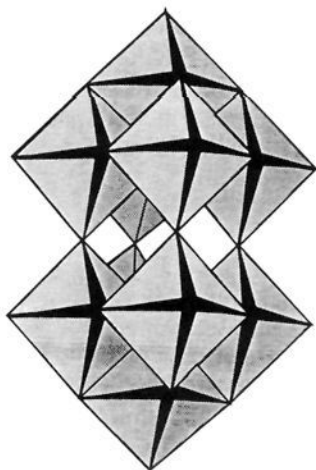
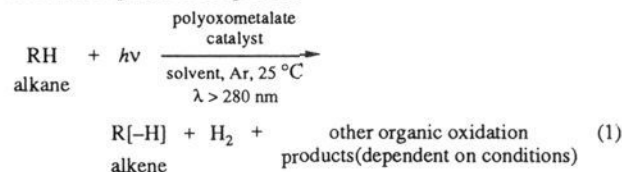


Figure 1. Structure of decatungstate, $W_{10}O_{32}^{4-}$, in polyhedral notation. **1** is the tetrakis(tetra-*n*-butylammonium) salt of this complex ($Q_4W_{10}O_{32}$). The two halves of this D_{4h} molecule are connected by four nearly linear $W^{VI}-O-W^{VI}$ bridges. In polyhedral notation, each octahedron represents one MO_6 unit; the oxygen atoms are the vertices of the octahedra, and the metal atoms are not directly seen.

to define photophysical or photochemical processes of novelty or potential utility lies in the fact that the soluble polyoxometalates have an extensive photochemistry under anaerobic conditions while the insoluble semiconductor metal oxides do not.⁶ Some applications of this polyoxometalate photochemistry include several unusual or unprecedented catalytic transformations of alkane substrates,⁵ new processes for deep-UV photomicroolithography,⁷ the catalytic selective dehalogenation of halocarbon toxins,⁸ and possible uses in fuel cell and other technologies. The development of rational methods for the experimental modulation of photoredox, thermal redox, and other features of polyoxometalates and semiconductors alike is of significant importance, and several efforts in this direction have been made with both types of materials.^{1,2,9,10} Of central interest here is the effect of surface protonation on the photochemistry of semiconductor metal oxides, phenomena addressed theoretically and experimentally in only a few papers.^{2d,11} While the point of zero charge can be used to evaluate the effects of protonation on semiconductors, extensive experimental delineation of these effects has not been possible because the materials are insoluble. Although definitive spectroscopic, X-ray crystallographic, and titration work has addressed the protonation of some polyoxometalates under static and stoichiometric conditions,^{1,12-14}

work addressing protonation of polyoxometalates under key dynamic, catalytic, and photochemical conditions is lacking. We report here a thorough study of the effect of protonation on the fundamental photoredox and related physical characteristics of one exemplary polyoxometalate, the tetra-*n*-butylammonium salt of decatungstate ($W_{10}O_{32}^{4-}$), **1** (Figure 1). This isopolytungstate complex is analogous to WO_3 , and in particular the cubic modification of this semiconductor.¹⁵ The photooxidation of alkanes, eq 1, was chosen for selected mechanistic probes in conjunction with this work as it is a fairly well understood polyoxometalate-facilitated photoredox process.⁵



Experimental Section

Materials. The polyoxometalates $Q_4W_{10}O_{32}$,¹⁶ **1**, $Na_4W_{10}O_{32} \cdot nH_2O$,^{5c} and $\alpha\text{-H}_3PW_{12}O_{40} \cdot nH_2O$ ^{17a} were prepared by literature methods. Q represents the tetra-*n*-butylammonium cation. The acetonitrile solvent (Burdick and Jackson glass-distilled grade) was used as received and stored under extra-dry argon. The alkanes were reagent grade from Wiley, Fluka, and Aldrich and had purities >99.9% by gas chromatography (GC). Nearly all of the organic products investigated were commercially available in high purity (>97%). The following reagent-grade acids were used: trifluoroacetic (TFA) (Aldrich), trifluoromethanesulfonic or triflic (Aldrich), perchloric (Mallinckrodt; 70% aqueous solution), and hydrochloric (Fisher; 12 N).

General Procedures. The UV-vis, GC, GC/MS, NMR, and IR data were collected as previously described.⁵ As before, deaerated acetonitrile solutions consisting of ~ 1.8 mM **1** and ~ 0.5 M alkane substrate were irradiated at 25 °C with an Oriol ozone-free (245-nm cutoff) 1000-W Xe arc lamp assembly. Electrochemical measurements were obtained in acetonitrile by cyclic voltammetry with concentrations of **1** similar to those used in the photochemical experiments.^{5c} The working electrode was a glassy carbon disc (BAS) with a surface area of 0.07 cm², the reference electrode was Ag/AgNO₃ in acetonitrile containing *n*-Bu₄N⁺PF₆⁻ (TBAPF₆), and the counter electrode was a platinum wire. The solutions for all the voltammetric measurements were degassed with argon. Control experiments were conducted with only the acids present in acetonitrile solvent. The potentials are formal potentials, E' , estimated as $(E_p + E_{pa})/2$, and are reported relative to Ag/AgNO₃(CH₃CN). The effects of acid on **1** in acetonitrile solvent were analyzed by ¹⁸³W NMR with the tetra-*n*-heptylammonium salt; only it was sufficiently soluble to render the measurements possible. The ¹⁸³W NMR spectra were obtained at 8.34 MHz in CD₃CN solutions in Wilmad 515-7PP 15-mm-i.d. NMR tubes with a probe temperature of 25 °C and were referenced to external 2.0 M Na₂WO₄ in D₂O. The equatorial and apical tungsten resonances characteristic of **1** were the only ones observed when the concentration of acid was varied, indicating the complex was not decomposing over the course of the experiments (see Figure 1S in the supplementary material).

Electron paramagnetic resonance (EPR) measurements (X band) were employed to determine further the species generated in the photoredox phenomena in question—polyoxometalate reduction and alkane oxidation—over a range of conditions. A Bruker ER 200-D-SRC spectrometer, equipped with a continuous flow cryostat (Oxford Instruments ESR 910) was used in all experiments. In a typical experiment, an acetonitrile solution, 0.4 M in cyclooctane and 3.34 mM in **1**, was placed in an EPR tube (Wilmad Glass Co., Inc.; No. 711-SQ-250m) and degassed. The tube was then placed in a special dewar flask (Wilmad No. WG-850) that facilitated direct irradiation of the contents of the tube while thermostated at various temperatures ($T = 23$ °C for most of the

(6) Nearly all reported processes involving the photochemical oxidation of organic substrates by semiconductor metal oxides have been run under an atmosphere of O₂.² Considerable work in our laboratory with Degussa P25 TiO₂ (anatase), generally considered to be one of the most effective semiconductors for photooxidation of organic materials, indicated little if any reaction with a variety of substrates in the absence of O₂: (a) Chambers, R. C.; Hill, C. L. *Inorg. Chem.* **1991**, *30*, 2776. (b) Chambers, R. C.; Renneke, R. F.; Hill, C. L. Unpublished work.

(7) (a) Heller, A. and co-workers, patents pending. (b) Okamoto, H.; Iwayanagi, T.; Mochiji, K.; Umezaki, H.; Kudo, T. *Appl. Phys. Lett.* **1986**, *49*, 298. (c) Kudo, T.; Ishikawa, A.; Okamoto, H.; Miyauchi, K.; Murai, F.; Mochiji, K.; Umezaki, H. *J. Electrochem. Soc.* **1987**, *134*, 2607. (d) Okamoto, H.; Ishikawa, A.; Kudo, T. *J. Photochem. Photobiol.* **1989**, *49*, 377.

(8) (a) Sattari, D.; Hill, C. *J. Chem. Soc., Chem. Commun.* **1990**, 634. (b) Sattari, D.; Hill, C. Unpublished work. The thermal reductive dehalogenation of CBr₄ by reduced heteropolytungstates has been reported by Ebersson and Ekstrom (*Acta Chem. Scand.* **1988**, *B42*, 101).

(9) Argitis, P.; Papaconstantinou, E. *Inorg. Chem.* **1986**, *25*, 4386.

(10) (a) Prosser-McCartha, C. M.; Kadkhodayan, M.; Williamson, M. M.; Bouchard, D. A.; Hill, C. L. *J. Chem. Soc., Chem. Commun.* **1986**, 1747. (b) Hill, C. L.; Bouchard, D. A.; Kadkhodayan, M.; Williamson, M. M.; Schmidt, J. A.; Hilinski, E. F. *J. Am. Chem. Soc.* **1988**, *110*, 5471.

(11) Papers on protonation and points of zero charge of semiconductor metal oxides: (a) Parks, G. A. *Chem. Rev.* **1965**, *30*, 177. (b) Lyklema, J. *J. Colloid Interface Sci.* **1984**, *99*, 109. (c) Léaustic, A.; Babonneau, F.; Chemseddine, A.; Livage, J. *New J. Chem.* **1989**, *13*, 111. See also: (d) Ward, M. D.; White, J. R.; Bard, A. J. *J. Am. Chem. Soc.* **1983**, *105*, 27. (e) Dung, D.; Ramsden, J.; Grätzel, M. *Ibid.* **1982**, *104*, 2977. (f) Goodenough, J. B.; Manoharan, R.; Paranthaman, M. *J. Am. Chem. Soc.* **1990**, *112*, 2076. (g) References in 2d.

(12) Day, V. W.; Klemperer, W. G.; Maltbie, D. J. *J. Am. Chem. Soc.* **1987**, *109*, 2991.

(13) Day, V. W.; Klemperer, W. G.; Schwartz, C. *J. Am. Chem. Soc.* **1987**, *109*, 6030.

(14) Recent deprotonation studies: Finke, R. G.; Rapko, B.; Saxton, R. J.; Domaille, P. J. *J. Am. Chem. Soc.* **1986**, *108*, 2947.

(15) Siedle, A. R.; Wood, T. E.; Brostrom, M. L.; Koskenmaki, D. C.; Montez, B.; Oldfield, E. *J. Am. Chem. Soc.* **1989**, *111*, 1665.

(16) (a) Chemseddine, A.; Sanchez, C.; Livage, J.; Launay, J. P.; Fournier, M. *Inorg. Chem.* **1984**, *23*, 2609. (b) Boyer, M. *J. Electroanal. Chem.* **1971**, *31*, 441.

(17) (a) Wu, H. *J. Biol. Chem.* **1920**, *43*, 189. (b) Rocchiccioli-Deltcheff, C.; Fournier, M.; Franck, R.; Thouvenot, R. *Inorg. Chem.* **1983**, *22*, 207.

experiments), followed by sample irradiation for the varying lengths of time indicated in Figure 8. Subsequent to irradiation, the EPR tube was transferred directly to the EPR spectrometer cavity maintained at 8–10 K for recording of the spectrum at this temperature. Specific data acquisition parameters are given in the Figure 8 caption.

Product Analysis. Under anaerobic conditions, the decatungstate reduction and organic functionalization products were simultaneously monitored by UV and GC, respectively. The reaction vessels employed were cylindrical 1.0-mm-path-length quartz cuvettes equipped with a long-neck, Teflon stopcock, and a side arm that allowed the facile degassing of the 2.0-mL volumes used. All reactions were run in the absence of hydrogen evolution catalysts; thus, the decatungstate was photoreduced 2–3 orders of magnitude faster than the subsequent reduced form was reoxidized by the evolution of hydrogen gas.⁵ This allowed the photoreduced decatungstate products to accumulate and be readily and accurately monitored as a function of time by following the intense blue chromophores (see below) characteristic of these species. The time-dependent evolution of organic products was evaluated by two methods. In the first, several different samples were irradiated to various stages of reduction and the GC measurements were made at the end of each reaction. In the second method, several GC measurements were made at different times during the course of one reaction. The results from both methods were mutually consistent. The cuvette reaction apparatus was withdrawn from the light for the period during which the sample was taken (~1 min). Other procedures have been published elsewhere.⁵

Oxidative titrations of the product solutions of the maximally photoreduced acidified systems with either Fe^{III} or O₂ indicated two electrons per initial molecule of **1**, in accord with literature values.^{4i,18} A Beer's law analysis of a mixture provided the concentration of one- and two-electron-reduced decatungstate species in maximally photoreduced solutions containing between 0 and 2.5 equiv of added strong acids (see supplementary material, Figure 2S). The two equations, $A_1/b = x\epsilon_{1e,\lambda_1} + y\epsilon_{2e,\lambda_1}$ and $A_2/b = x\epsilon_{1e,\lambda_2} + y\epsilon_{2e,\lambda_2}$, can be solved simultaneously for the unknowns x and y , which represent the concentrations of the one-electron- and two-electron-reduced decatungstate complexes, respectively, where A_i = the total absorbance at the wavelength λ_i ($i = 1$ or 2), b = path length of the cell (1 mm), ϵ_{1e,λ_i} = the extinction coefficient of the one-electron-reduced species at the wavelength λ_i ($i = 1$ or 2), and ϵ_{2e,λ_i} = the extinction coefficient of the two-electron-reduced species at the wavelength λ_i ($i = 1$ or 2). The one-electron-reduced decatungstate, $W_{10}O_{32}^{\cdot-}$, possesses an absorption maximum at 780 nm with a molar extinction coefficient, $\epsilon_{780,1e}$, of $\sim 7500 \text{ M}^{-1} \text{ cm}^{-1}$.^{5d,16} The two-electron-reduced species, $W_{10}O_{32}^{2-}$, has a maximum at 622 nm with $\epsilon_{622,2e} = 15\,500 \text{ M}^{-1} \text{ cm}^{-1}$.^{4i,5e,16} The concentrations obtained in this manner correlate with voltammetric and EPR data (see Results).

Due to the absence of hydrogen evolution catalysts, all the photochemical reactions given in this report are stoichiometric in decatungstate, effectively terminating when the decatungstate becomes maximally reduced. Under these conditions, the redox balance between the organic oxidation products and decatungstate reduction products could be determined accurately and were found to be high when alkanes were present (see Results). In the absence of alkane substrates, the decatungstate was photoreduced at appreciable rates; most of the organic products resulting from the loss of these electrons to the polyoxometalate were not detected. Succinonitrile, derived from the photooxidation of acetonitrile, was only observed in trace amounts.¹⁹ The products 1-butene and tributylamine, derived from **Q**, were detected in the absence of alkane substrate and in small quantities in the presence of various alkanes. These products do not result from a net redox reaction and hence do not lead to the net reduction of decatungstate. The similar rate behavior and product distributions observed with $Q_4W_{10}O_{32}$ and $Na_4W_{10}O_{32}$ in the photoreactions with and without acid additives or alkane substrates indicate that the potentially oxidizable Q^+ counterions are not involved to a significant extent in the photochemistry.

Employing deuterated acetonitrile had no effect on the quantum yields for photoreduction of **1**, with and without the presence of either alkane substrate or acid. Control reactions were run with 50:50 mixtures of CD_3CN/CH_3CN to cancel out effects caused by small differences in the

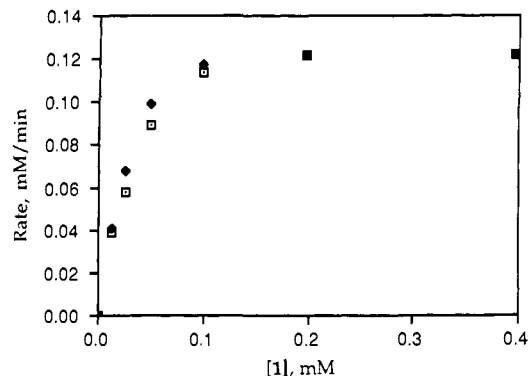


Figure 2. Experimental (□) and calculated (◆) initial rates of photo-reduction of **1** for the photochemical functionalization of cyclooctane as a function of the concentration of **1** for an exemplary acidified system. For the last two points, the experimental and calculated coincide exactly. [Cyclooctane] = 0.48 M, [triflic acid] = 10 mM, solvent = acetonitrile, and irradiation wavelength = 322 nm.

constituency of the solvent (water content, etc.). The cyclooctane reactions run in CD_3CN showed no apparent increase in the intensity of the CHD_2CN ¹H NMR resonance (quintet, δ 1.93), indicating any intermediates derived from reaction of the excited state with acetonitrile did not abstract hydrogen atoms from cyclooctane.

The photochemical and thermal stabilities of potential cyclooctane- and cyclohexane-derived functionalization products were analyzed under the reaction conditions. In a typical experiment, 1 equiv (based on **1**) of authentic samples of these potential products was added to the standard acidified and nonacidified solutions and the stability of each assessed by GC as a function of time either in the dark or under illumination. Thermally, the potential products did not react appreciably in any of these control reactions. Photochemically, they did not react appreciably under acidic conditions but did under the nonacidic conditions, where alkenes yielded either dimeric products or polymers, and alcohols yielded ketones. Subsequent reactions of the alkene products were quite pronounced in the cyclohexane photooxidation reactions but almost negligible in the cyclooctane photooxidation reactions, the reactions examined in greatest detail in this report. In the photochemical functionalization of both cyclic alkanes and 2,3-dimethylbutane by **1**, no alcohol was initially generated under the reaction conditions in any of the systems studied, including the acidified systems. Independently it was determined that the hydration of alkenes to alcohols was negligible under the reaction conditions. Care was taken to ensure that alcohols did not dehydrate and that alkenes did not isomerize in the hot injector port of the gas chromatograph. Extraction of the photolyte in the acidified reactions with *n*-pentane resulted in reproducible and reliable GC measurements, provided the injector port packing material (2% OV-101 on 100/120 mesh Chromosorb W-HP) had been recently replaced. The GC signals for alkenes disappeared immediately and completely upon the addition of small quantities of bromine along with the orange-brown color characteristic of the bromine. Cyclooctene formation in both the acidified and nonacidified systems was corroborated by ¹H NMR. No trifluoroacetate ester was indicated by GC or ¹H NMR for the cycloalkane reactions utilizing trifluoroacetic acid.

Rate Analysis. The quantum yields of photoreduction of **1** were determined at 265, 288, 322, and 354 nm by ferrioxalate actinometry using 1-cm rectangular quartz cuvettes.^{5d} The quantum yields are here defined as the moles of electrons present in the reduced decatungstate product per einstein of photons absorbed by the initially oxidized decatungstate. They were determined by using the standard procedure in which both the polyoxometalate and actinometer absorbed >99.9% of the incident light. The quantum yields and rates were derived from the nearly straight lines obtained at early times on plots of reduced decatungstate concentration versus time. In some cases, the decrease in the intensity of the chromophore associated with the oxidized species ($\lambda_{max} \approx 323 \text{ nm}$) was measured simultaneously for comparison. The dependence of the rates, $d[P_r]/dt$, where P_r = reduced polyoxometalate, on the concentration of decatungstate is shown in Figure 2 for irradiation with 322-nm light. These are approximately first-order at low concentrations, mixed-order at intermediate concentrations, and zero-order at high concentrations. Included in this figure for comparison are normalized calculated rates approximating the incident light as a δ -function at 322 nm. These were calculated from eq 2, where ϕ_{322} = quantum yield of photoreduction at

$$\left(\frac{d[P_r]}{dt} \right)_{322} = \phi_{322} I_a = \phi_{322} I_0 (1 - 10^{-\epsilon b c}) \quad (2)$$

(18) Significant uncertainties in the concentrations of the one- and two-electron-reduced species are inherent in this titration data because large uncertainties in the percentages can arise from much smaller uncertainties in the oxidative titer value of 1.7. If each decatungstate molecule were to be reduced by an average of only 1.5 electrons, then 50% of the molecules would be in the one-electron-reduced state and 50% in the two-electron-reduced state. Although the value of 1.7 from the titrations is within 13% of 1.5, the value of 30% obtained for the one-electron-reduced species at 1.7 is 60% smaller than the value of 50% obtained at 1.5.

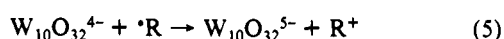
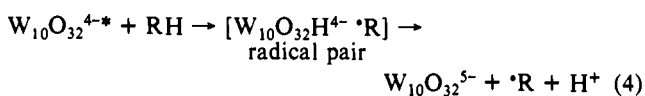
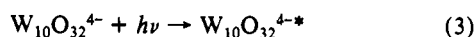
(19) Yamase, T.; Takabayashi, N.; Kaji, M. *J. Chem. Soc., Dalton Trans.* 1984, 793.

322 nm, I_a = the intensity of light absorbed at 322 nm, I_0 = the intensity of the incident light at 322 nm, $\epsilon = 14\,500\text{ M}^{-1}\text{ cm}^{-1}$ at 322 nm, b = path length of the reaction vessel (1 cm), and c = decatungstate concentration.

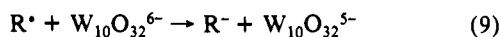
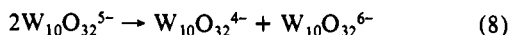
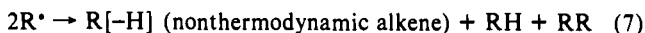
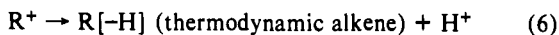
The rates for reoxidation of the reduced complexes by O_2 as a function of the concentration of added acid were obtained as follows. At each acid concentration, 2.0 mL of a deaerated acetonitrile solution with $[1] = 3.0\text{ mM}$ and $[\text{cyclooctane}] = 0.48\text{ M}$ were irradiated in a 1.0-mm-path-length cylindrical quartz cuvette until the photoreaction had attained 50% completion. At this time, the irradiation was stopped and to the cavity ($\sim 5\text{ cc}$) above the solution enclosed by the vessel was added 0.4 cm^3 of air. The vessel was then vigorously hand-shaken for $\sim 15\text{ s}$ to insure the rapid mixing of the added air and magnetically stirred for the remaining time required to monitor the reaction.

Results and Discussion

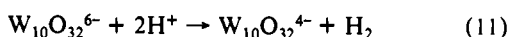
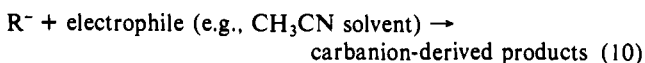
The addition of acids has a profound effect on the catalytic photochemical functionalization of alkanes by an exemplary redox active polyoxometalate, $\text{Q}_4\text{W}_{10}\text{O}_{32}$, **1**, eq 1. Several lines of spectroscopic and kinetics evidence presented and discussed here demonstrate that protonation of both ground- and excited-state decatungstate species substantially alters some of the general processes previously established to be operable in this chemistry, eqs 3–11.⁵ The acid dependence of several phenomena associated



(more important for more strongly oxidizing polyoxometalates than W_{10})



(only important for strongly reducing polyoxometalates)

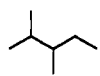
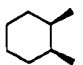


(H_2 evolution also seen from $\text{W}_{10}\text{O}_{32}^{5-}$)

with this chemistry, (1) quantum yields for alkane photooxidation, (2) polyoxometalate redox potentials, (3) rates of reoxidation of reduced catalyst, e.g., eq 11, (4) organic product distributions, (5) polyoxometalate UV-visible spectra, (6) reduced polyoxometalate product distributions, (7) polyoxometalate EPR spectra, (8) kinetics and rate behavior, and (9) other spectroscopic and chemical processes, are all mutually consistent with one another and all reach limiting values at ~ 2.5 equiv of triflic acid/equiv of **1**. Higher quantities of the weaker acids, such as trifluoroacetic and HCl, are required to attain the limiting behavior in these experiments, whereas with the strong triprotic heteropoly acid $\alpha\text{-H}_3\text{PW}_{12}\text{O}_{40}$, the limiting behavior is attained when only 0.6 equiv of the complex is added. Each of these lines of experimental evidence are elaborated sequentially below.

Quantum Yields. The quantum yields obtained at 322 nm under acidic and nonacidic conditions for photooxidation of the exemplary cyclic alkane substrates cyclooctane and cyclohexane and the exemplary branched alkane substrates 2,3-dimethylpentane and *cis*-1,2-dimethylcyclohexane by **1** are given in Table I. The addition of strong to moderate acids increases the quantum yields for these processes from ~ 0.1 to ~ 1 . For the slower nonacidified systems with quantum yields of ~ 0.03 , this represents a 25-fold increase! The protons and not the conjugate bases influence the photochemistry, as indicated by the constancy of the limiting

Table I. Quantum Yields for the Photochemical Functionalization of Cyclic and Branched Alkanes by **1** in the Presence and Absence of Acids^a

alkane	acid	[acid] ^b	quantum yield ^c
cyclooctane	none	0	0.16
	trifluoroacetic (TFA)	470	1.00
	hydrochloric	7.88	0.95
	perchloric	10.44	1.06
	triflic	7.88	1.09
	$\alpha\text{-H}_3\text{PW}_{12}\text{O}_{40}$	1.23	1.07 ^d
cyclohexane	none	0	0.02
	TFA	470	0.53
	none	0	0.03
	triflic	4.04	0.72
	none	0	0.04
	triflic	4.11	0.92

^a Conditions: $[1] = 1.8\text{--}3.3\text{ mM}$, $[\text{alkane}] = 0.48\text{ M}$ in acetonitrile solvent under an inert atmosphere. Irradiation with a 322-nm interference filter at $25\text{ }^\circ\text{C}$. ^b Equivalents of acid per equivalent of **1**. ^c Values at 322 nm. ^d Obtained upon considering the relative amount of light absorbed by $\alpha\text{-H}_3\text{PW}_{12}\text{O}_{40}$ and **1** at the wavelength of irradiation.

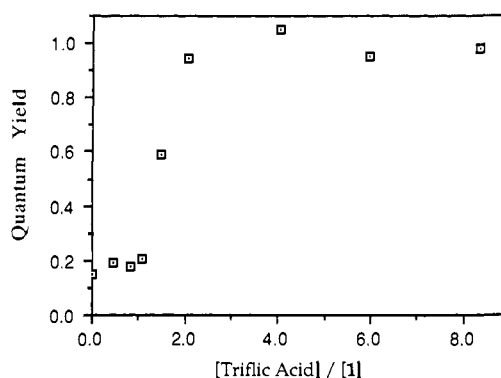


Figure 3. Quantum yields of photoreduction of **1** by cyclooctane substrate as a function of the ratio of the concentration of triflic acid to that of **1**. $[1] = 1.8\text{ mM}$, $[\text{cyclooctane}] = 0.48\text{ M}$, solvent = acetonitrile, and irradiation wavelength = 322 nm, throughout.

quantum yields of ~ 1 for a range of acids, including the oxidatively resistant $\alpha\text{-H}_3\text{PW}_{12}\text{O}_{40}$. In Figure 3, the quantum yields for photoreduction of **1** with cyclooctane substrate are seen to approach values of ~ 1 when 2 equiv of triflic acid has been added. These values were obtained at early times before the solution had been photoreduced by more than 5%. The isotope effect for photooxidation of the substrates cyclohexane- d_{12} and cyclohexane- h_{12} by **1** was determined to be 2.5 either *in the absence or in the presence of acid*, a value consistent with several mechanisms for the substrate activation processes in the mechanism. Thorough previous studies of the mechanism of photooxidation by polyoxotungstates in the absence of acid argue strongly that the substrate activation process involves rate-determining atom abstraction (H transfer) to the polyoxometalate excited state when the substrates are alkanes, eq 4.⁵

Cyclic Voltammetry and Ground-State Redox Potentials. The redox potentials of **1** were measured by cyclic voltammetry (Figure 4).²⁰ The first reduction wave increases by 1 V upon the addition of acid! The voltammograms are quasi-reversible and consist of two one-electron waves (formal potential, $E^f = -1.2$ and -1.8 V vs Ag/AgNO_3) for the nonacidified system and one quasi-reversible two-electron wave ($E^f = -0.1\text{ V}$) for the acidified system (acid is 4 equiv of HClO_4 /equiv of **1**).²¹ The peak-to-peak

(20) The affect of acid on the cyclic voltammetric behavior of some polyoxometalates has been reported: Keita, B.; Nadjio, L. *J. Electroanal. Chem.* 1987, 227, 77.

(21) The two-electron wave might be a near superposition of two one-electron waves. This point was not pursued further by differential pulse polarography or other methods.

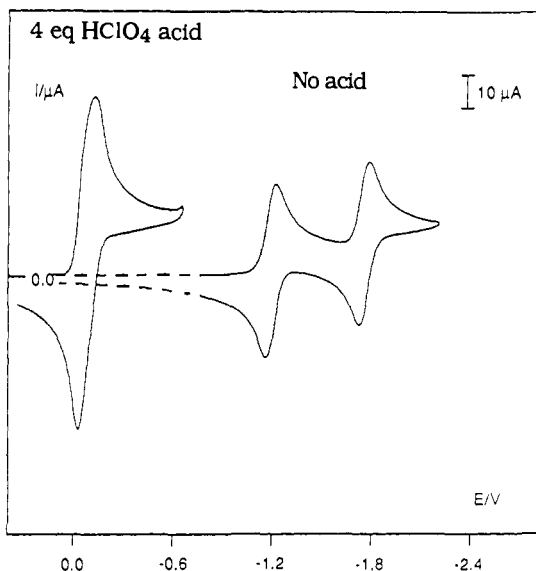


Figure 4. Cyclic voltammograms of **1** for systems containing 4 equiv of perchloric acid/eq of **1** and no added acid. The formal potentials, E^f , and peak-to-peak separations are given in the text. There are no polyoxometalate-based redox waves in the absence of acid where the wave under acidic conditions appears, and there are no polyoxometalate-based redox waves in the presence of acid where the waves under neutral conditions appear. $[1] = 1.7 \text{ mM}$, solvent = acetonitrile, supporting electrolyte = 0.1 M TBAPF_6 , scan rate = 100 mV/s , and $T = 25 \text{ }^\circ\text{C}$.

potential difference, $E_{pc} - E_{pa}$, is 100, 90, and 200 mV for the two waves of the unprotonated species and the protonated species, respectively. Similar voltammetric behavior is seen with either perchloric or triflic acid. The voltammetric data were obtained under conditions resembling as closely as possible those employed in the reactions involving alkane photooxidation by **1**. In addition, the peak current potentials (E_{pc}) for electrochemical reduction of **1** were determined as a function of added triflic acid; limiting behavior is seen at ~ 2 equiv of acid/eq of **1** (Figure 3S in the supplementary material).

Reoxidation of Reduced Catalysts, Equation 11. The rate of reoxidation of the reduced form(s) of the catalyst either by H_2 evolution, eq 11, or O_2 oxidation, and not the rate of generation of reduced polyoxometalate, eqs 3 + 4 and 5, usually limits the rate of overall catalytic recycling in alkane photooxidation by polyoxometalates.⁴⁵ Solely on the basis of redox potentials, one would expect that the acid dependence of reduced polyoxometalate generation would be the opposite from that of reduced polyoxometalate reoxidation. Experimentally this is found to be the case. A significant decrease in the rate of reduced decatungstate reoxidation by O_2 results upon acidification, which parallels the changes in the ground-state redox potentials. Similar correlations between polyoxometalate reoxidation rates and their reduction potentials have been reported.^{4a,22} The protons introduced into the systems containing **1** by the addition of acids do not facilitate the evolution of hydrogen gas from the reduced species even when hydrogen evolution catalysts such as Pt^0 and RuO_2 are present. Instead, the reoxidation rate obtained in the presence of these catalysts is ~ 10 -fold slower for the acidified systems than the nonacidified systems, reflecting again, the dominant effect of polyoxometalate protonation. Although the addition of Pt^0 allows for the rapid reoxidation of the reduced **1** species in the absence of acid additives and efficient catalytic turnover (200 cycles obtained after 4 h or irradiation with $<5\%$ decomposition of **1** indicated by UV-vis), this is not the case for the acidified systems. The rate of reoxidation of reduced **1** by O_2 has been determined as a function of the concentration of triflic acid ($[\text{triflic acid}]/[1]$) (Figure 4S). The rate begins to drop off rapidly at less than 0.2 equiv of H^+ /equiv of reduced **1**, and again, limiting behavior is seen at above 2 equiv of H^+ .

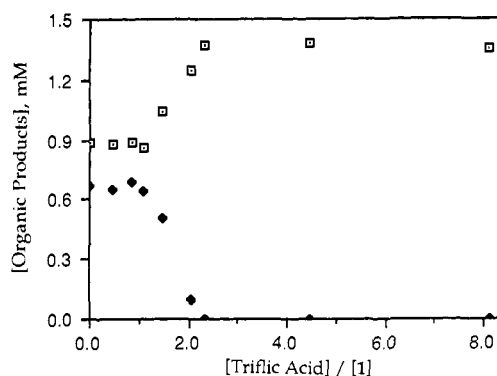


Figure 5. Concentrations of cyclooctene (\square) and bicyclooctyl (\blacklozenge) obtained from the photochemical functionalization of cyclooctane by **1** as a function of the concentration of triflic acid (ratio of concentration of triflic acid to **1**). At the time the measurements were made, **1** was maximally photoreduced. $[1] = 1.8 \text{ mM}$, [cyclooctane] = 0.48 M , and solvent = acetonitrile.

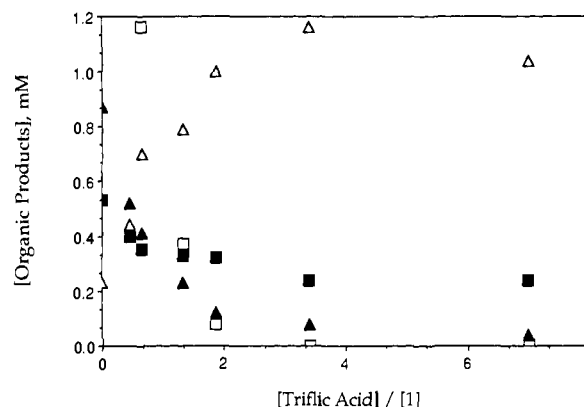


Figure 6. Concentrations of *trans*-1,2-dimethylcyclohexane (\square), 2-methylcyclohexenylidene (\blacktriangle), 1,6-dimethylcyclohex-1-ene (\blacksquare), and 1,2-dimethylcyclohexene (\triangle) obtained from the photochemical functionalization of *cis*-1,2-dimethylcyclohexane by **1** as a function of the concentration of triflic acid. At the time the measurements were made, **1** was maximally photoreduced. $[1] = 1.8 \text{ mM}$, [cyclooctane] = 0.48 M , and solvent = acetonitrile.

Alkane-Derived Products. The organic product distributions for the photooxidation of cyclic and branched alkane substrates by **1** obtained under both nonacidic and acidic conditions are given in Table II. For nonacidified systems, cyclic alkane substrates yield cycloalkene and bicycloalkyl (methyl ketone is observed with cyclohexane), whereas branched alkane substrates yield a nonthermodynamic mixture of alkenes, with the major products being the α -olefins. For the acidified systems, cyclic alkane substrates yield only cycloalkenes, whereas branched alkane substrates yield a mixture of alkenes, with the major product being the tetra-substituted olefin. The branched alkenes obtained from the acidified branched alkane substrates do not arise from an acid-catalyzed isomerization at the temperatures employed in these particular reactions, $0 \text{ }^\circ\text{C}$. The redox balance between electrons in the reduced decatungstate species and oxidized organic products is reasonably high for all the reactions shown. The detected products for all nonacidified reactions account for $>85\%$ of the redox equivalents in the reduced decatungstate. For the acidified systems, this value varies between 75% for cyclooctane and 55% for cyclohexane.

In Figure 5, it is evident that, for reactions with cyclooctane substrate, the product cyclooctene forms at the expense of bicyclooctyl when between 1 and 2.5 equiv of triflic acid is added/eq of **1**; limiting behavior is attained at 2.5 equiv of acid. The distributions in Figure 5 (and Figure 5S in the supplementary material) were collected for maximally photoreduced systems. For cyclooctane substrate, small changes in both the values of the quantum yields and the relative quantities of alkene and dimer are observed when less than 1 equiv of acid has been added. The

Table II. Organic Product Distributions from the Photochemical Functionalization of Cyclic and Branched Alkanes by **1** in the Presence and Absence of Acids^a

system ^b	organic products ^c						redox balance ^d
Substrate = cyclooctane (○)							
(1) H ⁺	>99	0	0	0	0	0	80
(2) no H ⁺	55	45					>90
Substrate = cyclohexane (○)							
(3) H ⁺	>99	0	0	0	0	0	50
(4) no H ⁺	25	32	37				90
Substrate = <i>cis</i> -1,2-dimethylcyclohexane (○)							
(5) H ⁺	79	18	<3	0	0	0	83
(6) no H ⁺	4	12	19	55			90
Substrate = 2,3-dimethylpentane (—)							
(7) H ⁺	55	26	7	9	3	~0	68
(8) no H ⁺	~0	5	<2	61	9	10	85

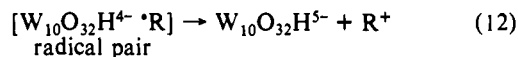
^a Conditions: [1] = 1.8 mM, [alkane] = 0.48 M in acetonitrile solvent under an inert atmosphere. $T = 25\text{ }^{\circ}\text{C}$ for all the reactions except those containing branched alkanes and acid, reactions 5 and 7. These were run at $T = 0\text{ }^{\circ}\text{C}$ to prevent the acid-catalyzed thermal isomerization of alkenes subsequent to their formation. The distributions shown represent maximally photoreduced systems. To achieve this state, the acidified and nonacidified systems generally required ~ 5 and ~ 30 min of irradiation, respectively ($\lambda > 295\text{ nm}$). ^b "H⁺" represents a system acidified with ~ 4 equiv of triflic acid/quiv of **1** and "no H⁺" represents a system to which no acid has been added. ^c The numbers given represent the moles of the corresponding organic product divided by the total number of moles of all organic products detected by GC. ^d Yields given are the equivalents of electrons represented by the sum of the organic oxidation products reported divided by the equivalents of electrons in the photoreduced decatungstate.

behavior exhibited by the branched alkane substrates 2,3-dimethylpentane and *cis*-1,2-dimethylcyclohexane is slightly different from that exhibited by cyclooctane. Figure 6 and Figure 6S in the supplementary material show, respectively, that the organic product distributions and quantum yields begin to change well before 1 equiv of triflic acid has been added and limiting values are reached at ≥ 2 equiv of H⁺/equiv of **1**. In these cases, the quantum yields start to increase and the organic product distributions start to show an increase in the ratio of maximally to minimally substituted olefins and, for the *cis*-1,2-dimethylcyclohexane reactions, a decrease in the isomerization reaction yielding *trans*-1,2-dimethylcyclohexane.

The observed alkane-derived products seen in these studies are consistent with our knowledge of the energetic and mechanistic features of catalytic photochemical functionalization of alkanes by polyoxotungstate from previous studies, eqs 3–11,⁵ and with the dependence of the redox potentials of **1** on added acid (vide supra). In sharp contrast to the nonacidified solutions of decatungstate, where freely-diffusing alkyl radical intermediates are not appreciably oxidized by oxidized decatungstate,^{5c} alkyl radical intermediates are readily oxidized to carbocations by acidified solutions of the complex. That is, eq 5 is facile for the protonated complex. This is indicated by the dominance of the most substituted alkene products, obtained from photooxidation of the branched alkane substrates, and the absence of dimer radical coupling products, obtained from photooxidation of the cyclic

alkane substrates. An alkene product distribution highly enriched in the most substituted isomers should arise from the deprotonation of a tertiary carbocation in accord with Zaitsev's rule.²³ Tertiary radicals, derived from branched alkane substrates, are expected to be more readily oxidized by decatungstate than the more weakly reducing secondary radicals, derived from cyclic alkane substrates, points also in accord with the detected organic products. At limiting concentrations of acid ($[\text{H}^+]/[\mathbf{1}] > 2$), where the maximally protonated complexes are present, both secondary and tertiary radicals are readily oxidized.

The two most likely modes of radical oxidation involve diffusion of the initially formed radical out of the cage followed by oxidation by a second molecule of oxidized decatungstate (eqs 4 and 5), or direct oxidative transfer of the second electron from the radical to the one-electron-reduced complex while both are still in the radical pair (eq 12). The EPR data coupled with the UV-visible



data discussed below indicate, however, that the net two-electron process (eq 12) is not likely. Under acidic conditions, $S = 1/2$, one-electron-reduced species are initially generated followed only by a slower disproportionation of these species into $S = 0$ oxidized and two-electron-reduced complexes.

Evidence from Electronic Absorption Spectra. Distinct distributions of photoreduced forms of **1** are indicated by characteristic bands in the visible region of the spectrum.²⁴ Two features in the electronic absorption spectra of **1**, in the absence and presence of acid, are significantly distinct: (1) the shape of the lowest energy ligand-to-metal charge-transfer (LMCT) bands in the oxidized species and (2) the shape of the absorption bands in the photoreduced species that give rise to its intense blue color. These are shown in Figure 7, which illustrates the spectra obtained as a function of irradiation time for both types of systems. For these, the lowest energy LMCT band decreases in intensity as the visible band increases until the lowest energy LMCT band is apparently absent in highly reduced solutions. For the oxidized species, the addition of acid causes the λ_{max} of the lowest energy LMCT band to blue shift from 326 to 319 nm and the intensity of this band to decrease from $\epsilon_{326/\text{no H}^+} = 14\,500\text{ M}^{-1}\text{ cm}^{-1}$ to $\epsilon_{319/\text{H}^+} = 13\,500\text{ M}^{-1}\text{ cm}^{-1}$. The second lowest energy band also shows some decrease in intensity. The isosbestic points noted in the spectra of the oxidized complex as the concentration of acid is varied indicate only two species are present as the acid concentration is varied (Figure 7c). Resonances arising from polyoxotungstate decomposition products are not observed by ¹⁸³W NMR, indicating other species do not give rise to the changes in the UV-vis absorption spectra. No changes in the LMCT absorption bands of **1** in the absence of acid result after addition of some of the salts of the acids utilized, such as sodium trifluoroacetate, and upon the addition of large quantities of water or polar aprotic solvents such as DMF.²⁵ The initial spectrum of the oxidized species is regenerated upon addition of small quantities of mildly basic species including H₂O ($\text{p}K_{\text{a}} \approx -1.6$), amines ($\text{p}K_{\text{a}} \approx 10$), or sodium bicarbonate ($\text{p}K_{\text{a}} \approx 6$) within the time of mixing (seconds) (Figure 7S in the supplementary material). Such large changes in the LMCT bands of the oxidized decatungstate species are not observed upon the addition of other electrolytes, although changes in the spectrum of the reduced species can change considerably by varying the solvent. Like the UV-vis spectrum, the

(23) Zaitsev's rule states that a carbonium ion intermediate with more than one type of β -hydrogen will undergo E1 elimination to generate the most stable alkene (an approximately thermodynamic distribution of alkenes); cf. March, *J. Advanced Organic Chemistry*, 3rd ed.; Wiley: New York, 1985; p 889.

(24) It has been noted that the equilibrated distribution obtained photochemically or electrochemically is dependent on solvent and that reduction by more than two electrons is not possible photochemically.¹⁶

(25) Addition of much greater quantities of water ($\sim 50:50$ water/acetonitrile) can lead toward the gradual decomposition of **1**. Decomposition induced in this manner occurs at a slow rate that depends on the temperature. In contrast, the change in the UV spectrum induced by the addition of acid is instantaneous and independent of temperature.

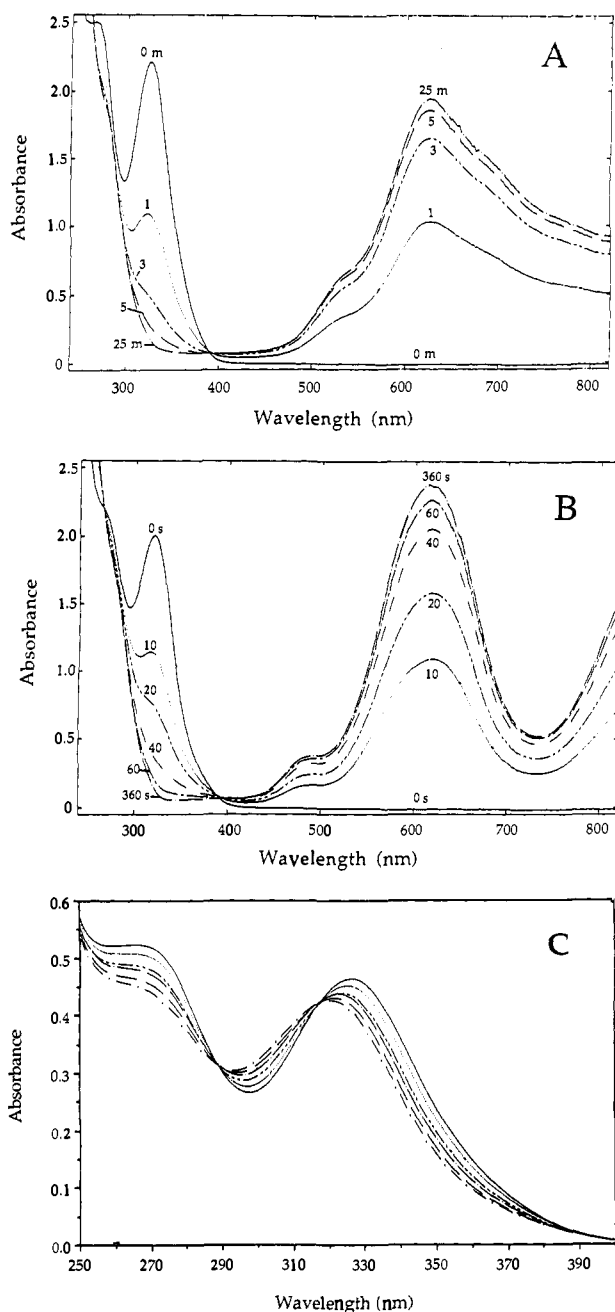


Figure 7. UV-vis spectra of **1** for the photochemical functionalization of cyclooctane as a function of irradiation time: (A) a system containing no acid (0–25 min); (B) a system containing 3 equiv of triflic acid/quiv of **1** (0–360 s), $[1] = 1.5$ mM, $[\text{cyclooctane}] = 0.48$ M, solvent = acetonitrile, and optical path length = 1.0 mm; (C) UV spectra of the lowest energy LMCT bands of oxidized **1** obtained upon increasing the concentration of triflic acid: 0 (—), 0.22, 0.58, 0.77, 1.12, and 2.12 (---) equiv of triflic acid/quiv of **1**, $[1] = 3.35$ mM, solvent = acetonitrile, and optical path length = 0.10 mm.

^{183}W NMR spectrum reverts to the original upon the addition of bases.

Excited-state redox potentials usually correlate with ground-state redox potentials, and excited states are almost always more potent oxidizing agents, thermodynamically and kinetically. The modest perturbations of the electronic absorption spectral features as a function of protonation indicate that the HOMO–LUMO gap, an analogy in molecular systems to the band gap in semiconductors, is modestly perturbed at most upon protonation. Given the ground-state redox potentials above, the excited state of the protonated complex is ~ 1 V more oxidizing than the excited state of the unprotonated complex to a first approximation.

An equation, including protons for generality, describing the photoreduction of nonacidified and acidified solutions of **1** is given

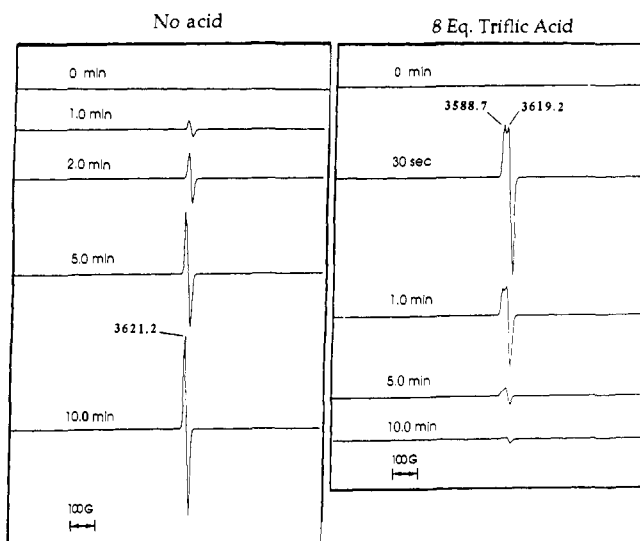
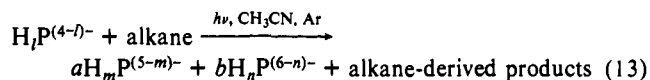


Figure 8. EPR spectra of reduced decatungstate species generated upon irradiation of **1** in acetonitrile solutions of cyclooctane substrate without (left column) and with (right column) 8 equiv of triflic acid/quiv of **1**. All irradiations were carried out at 23 °C for the time intervals given on each spectrum above. All spectra were then recorded at 8–10 K with the same instrumental data collection parameters (power, 40 dB; gain, 4×10^4 , sweep width, 4000 G).

in eq 13. The number of protons H_l , H_m , and H_n associated with the oxidized species $H_lP^{(4-l)-}$ and the one- and two-electron-reduced species $H_mP^{(5-m)-}$ and $H_nP^{(6-n)-}$, respectively, are indicated by the integers l , m , and n . The ratio b/a increases as the acidity of



the reduced solution increases. For the nonacidified system (Figure 7A), the asymmetric band in the visible region of the spectrum corresponds to $a = 0.3$ and $b = 0.7$ at all times. For the acidified system (Figure 7B), this band changes shape and is roughly Gaussian; it corresponds to $a \approx 0$ and $b \approx 1$ at all times. Protons arise in the photochemical systems directly from the alkane dehydrogenation process. In the nonacidified systems, the extra negative charge generated upon photoreduction by 1.7 electrons/molecule of **1** must be balanced by 1.7 protons/1. Protons do not arise in this manner for the systems reduced electrochemically where the tetra-*n*-butylammonium counterions balance the charge instead.^{16a} The values a and b at equilibrium are not solely dependent on the concentration of protons, however. Their dependence on the solvent has been documented.²⁶ For the oxidized species, like the reduced species, changes in the shape of the lowest energy LMCT bands are very pronounced between 0 and 2 equiv of added acid and level off at 4 equiv²⁷ (see Figure 7c).

Evidence from EPR Spectra. The EPR spectra of the photoreduced nonacidified and acidified systems illustrate or corroborate some points (Figure 8). First, the large attenuation in the signal near the photoreduction limit (at $t = 10$ min) indicates a large decrease in the ratio [one-electron reduced complex]/[two-electron reduced complex] upon addition of acid. The $S = 1/2$ one-electron-reduced complex is EPR active; the $S = 0$, antiferromagnetically coupled, two-electron-reduced complex is EPR silent.^{1a} Second, the series of EPR spectra in the presence of acid directly indicate the presence of two distinct one-electron-reduced intermediates. Although hyperfine coupling to protons has been reported before in the EPR spectra of reduced polyoxometalates,¹⁹ the change in the g values and the change in the difference between the g values (Δg) as a function of irradiation time strongly suggest

(26) Changes in the values of a and b have also been reported upon varying the solvent.¹⁶

(27) Dilution causes the intensity to decrease uniformly at all wavelengths, especially when large quantities such as 12.4 equiv of acid are added.

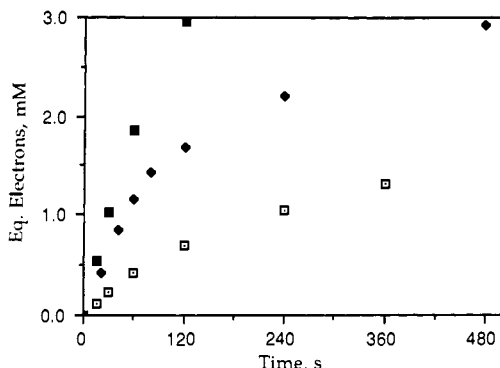


Figure 9. Reduction of **1** as a function of irradiation time for the photochemical functionalization of cyclooctane at three different acid concentrations: 0 (\square), 1.0 (\blacklozenge), and 3.0 (\blacksquare) equiv of triflic acid/quiv of **1**. $[\mathbf{1}] = 1.8$ mM, $[\text{cyclooctane}] = 0.48$ M, and solvent = acetonitrile. The extent of the reduction of **1** is given as equivalents of electrons per equivalent of **1**.

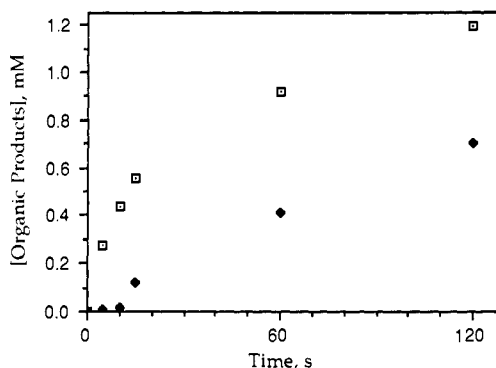


Figure 10. Concentrations of cyclooctene (\square) and bicyclooctyl (\blacklozenge) as a function of irradiation time obtained for the photochemical functionalization of cyclooctane with a system containing 1.0 equiv of triflic acid/quiv of **1**. $[\mathbf{1}] = 3$ mM, $[\text{cyclooctane}] = 0.48$ M, and solvent = acetonitrile.

that two EPR-active (i.e., one-electron-reduced decatungstate) forms are present under these conditions and not just one form exhibiting hyperfine coupling. Third, the similarity of the g values of the one EPR-active species in the absence of acid with the lower g value (higher field) species in the presence of acid (both ~ 3620 G) indicates that they are the same compound, leading to an assignment that this compound is $W_{10}O_{32}^{5-}$, and the other resonance in the presence of acid (~ 3589 G) is the monoprotonated compound $HW_{10}O_{32}^{4-}$. The acid dependence of the relative concentrations of one- and two-electron-reduced decatungstate species produced upon cyclooctane photooxidation, as indicated by EPR, are consistent with the data from the UV-visible and other spectra.

Rate Behavior. The results of several experiments summarized in this section confirm the validity of several processes in the mechanism, eqs 3–11, the presence of different protonation states of **1**, and the preferential uptake of protons by the more basic reduced forms of the complex. On the way to complete photo-reduction of **1**, for systems containing cyclooctane as the substrate, the decatungstate reduction and organic oxidation product distributions along with the reaction rates are found to vary with time in manners that are specific to a particular concentration of added acid. While the oxidized protonated species is present, it can contribute to the enhancement in quantum yield, as quantum yield is specifically defined in this study, by oxidation of the alkyl radical intermediates. As the oxidized protonated complex is depleted, quantum yield enhancement by oxidation of the alkyl radical intermediates tends toward the behavior obtained in its absence. The time-dependent plots of the equivalents of electrons contained in the reduced decatungstate complex and the organic oxidation products are shown in Figures 9 and 10, respectively, under particular conditions. Tangent lines to the curves in these plots correspond to the instantaneous rates at a particular time. Three distinct types of behavior are observed with regard to these properties as the amount of added acid is increased. The first type of behavior is observed in the absence of any acid. Under these conditions, a constant ratio of decatungstate reduction products (70% two-electron- and 30% one-electron-reduced species) and cyclooctane oxidation products (57% cyclooctene and 43% bicyclooctyl) is observed at all times. Similar behavior with regard to the organic and inorganic products and the quantum yields is observed between 0 and 1 equiv of added acid. The second type of behavior is observed upon the addition of between 1 and 2.5 equiv of strong acid. The clearly distinguishable symmetric spectrum attributable to the presence of solely the two-electron-reduced decatungstate is present at early reaction times (Figure 8S in the supplementary material). Cyclooctene appears as the predominant organic oxidation product during these times; very small quantities ($<1/10$ of the quantity of cyclooctene) of bicyclooctyl are present (see Figure 10). At later times, there is a gradual change in the spectrum attributable to an increase in the concentration of the one-electron-reduced complex along with

a rapid increase in the bicyclooctyl concentration. The product versus time plots show the greatest curvature at this acid concentration than at all the other concentrations studied. The initial rates are fast, resembling the acidified systems, and rapidly slowing toward those associated with the nonacidified system (see Figure 9). This biphasic behavior is not observed for systems containing quantities of added acid not compatible with the simultaneous presence of two protonation states, i.e., those containing 0 and greater than 2.5 equiv of acid. The third type of behavior is observed when greater than 2.5 equiv of strong acid are added. Under these conditions, the only spectrum is that of the two-electron-reduced decatungstate and the only organic oxidation product is cyclooctene and these are observed at all reaction times. The product versus time plots show little curvature until late reaction times, like the nonacidified reactions. Inner-filter effects are absent for this and all other decatungstate solutions studied, since the reduced forms of decatungstate do not compete with the oxidized forms for light absorption in the region of irradiation, simplifying the time-dependent analysis.

Several variables in addition to the acid concentration were systematically altered including the concentration of cyclooctane, the light intensity, and the concentration of **1**. The dependences of the initial quantum yields on the concentration of cycloalkane for the nonacidified and acidified (TFA) reactions show varying degrees of curvature and are more linear for the reactions displaying the lowest quantum yields (Figure 9S in the supplementary material). The nonacidified cyclohexane reactions are first-order in alkane throughout the concentration range in which cyclohexane is soluble. The acidified cyclohexane reactions show complex behavior as the concentration of alkane is varied. A limiting quantum yield is not attained even at the solubility limit of cyclohexane of 1.1 M. The acidified cyclooctane reactions show first-order kinetics at low concentrations and approximately zero-order kinetics at high concentrations where a limiting quantum yield of 0.95 is obtained. The nonacidified cyclooctane systems show less curvature than the acidified cyclooctane systems but more than the nonacidified cyclohexane systems, in accordance with their intermediate quantum yields.

The initial rates are first order in light intensity for both the nonacidified and acidified systems for the light intensities employed in these studies (Figure 10S in the supplementary material). This behavior was observed by using neutral density filters in conjunction with a 322-nm interference filter. Nearly constant quantum yields and organic oxidation product distributions are obtained as a function of wavelength for both the nonacidified and acidified systems. This is the case in spite of the fact that two different bands are irradiated to different degrees as the wavelength of irradiation is varied. The initial rates as a function of the concentration of decatungstate are directly related to the light absorption properties of the molecule for both the acidified and nonacidified systems, as discussed in the Experimental Section.

When these results are coupled with variations in the quantity of the polyoxometalate and the added acid, critical information

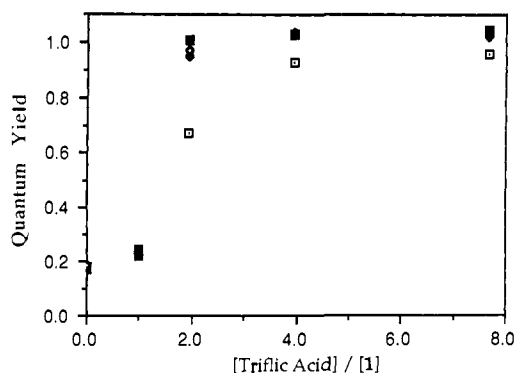
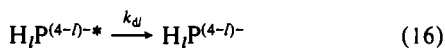
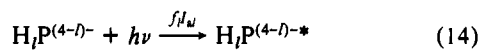


Figure 11. Quantum yields of photoreduction of **1** by cyclooctane substrate as a function of the concentration of triflic acid at four different concentrations of **1**: 0.124 mM (\square), 0.373 mM (\blacklozenge), 1.12 mM (\triangle), and 3.36 mM (\blacksquare). [Cyclooctane] = 0.48 M, solvent = acetonitrile, and irradiation wavelength = 322 nm. The [triflic acid] is given as equivalents of triflic acid per equivalent of **1**.

regarding the role of acids is obtained. Figure 11 shows that plots of rate vs [triflic acid] have similar shapes over a range of [1] varying by a factor of 27. A limiting rate is reached before 2.0 equiv of triflic acid has been added for all but the least concentrated decatungstate solution. These rates are equivalent for those concentrations analyzed, demonstrating optically dense conditions at 322 nm. Related to these experiments are the plots of rate versus [1] for systems acidified with trifluoroacetic acid (Figure 11S in the supplementary material). In both the presence and absence of alkane substrate, after light absorption has been maximized by increasing [1] to a sufficiently high enough level, a gradual decrease in the rate results upon further increasing the concentration of decatungstate at a constant acid concentration.

The manner in which protonation affects the processes directly associated with the excited state can be evaluated more quantitatively; eqs 14–16 can be written, where P = decatungstate moiety; superscripts designate charge, I_{al} = intensity of the light absorbed by the decatungstate species with l protons ($l = 0, 1$, or 2), f_l = quantum yield for production of the photochemically active excited state, k_l = rate constant for reductive quenching of excited state, k_{dl} = rate constant for nonradiative decay of excited state, and $l = k$ ($k = 1$ or 2). As in eq 13, l represents



the number of protons on the decatungstate; $l = 0$ for the nonprotonated species, and $l = k$ ($k = 1$ or 2) for the protonated species. Light absorption (eq 14) is followed by the reductive quenching of the excited state by the alkane substrate and the generation of an alkyl radical (eq 15). Nonradiative excited-state decay (eq 16) competes with the latter; luminescence has been detected in certain polyoxometalate systems but is far too low to be kinetically significant here.^{3,28}

A rate law (eq 17) in accord with all the experimental data can be formulated consisting of three factors, two of which relate to the excited state and the other to the ground state ($+d[P_r]/dt$ = rate of decatungstate reduction, including thermal reduction by alkyl radical intermediates, $[P^{4-}]_0$ = initial concentration of $W_{10}O_{32}^{4-}$, I_{aT} = the amount of light absorbed by all the decatungstate species, k_{ql} = total alkane quenching rate constant; other

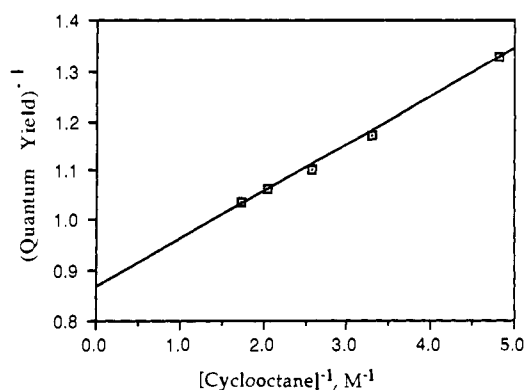


Figure 12. Double-reciprocal plot of quantum yields versus the concentration of cyclooctane for an exemplary acidified system. [1] = 1.8 mM, [TFA] = 0.8 M, solvent = acetonitrile, and irradiation wavelength = 322 nm. From a least-squares analysis, the slope = 0.095 and the y-intercept = 0.86.

terms defined for eqs 9–11; here $l = 0$ for the nonprotonated species, and $l = k = 1$ or 2 for the reactive protonated species).

$$\frac{+d[P_r]}{dt} = \alpha \left(\frac{[H_kP^{(4-k)-}]}{[P^{4-}]_0} \right) \left(\frac{f_k I_{aT} k_k [RH]}{k_{qk} [RH] + k_{dk}} \right) + \alpha \left(\frac{([P^{4-}]_0 - [H_kP^{(4-k)-}])}{[P^{4-}]_0} \right) \left(\frac{f_0 I_{aT} k_0 [RH]}{k_{q0} [RH] + k_{d0}} \right) \quad (17)$$

Steady-state expressions corresponding to the reactive protonated, $H_kP^{(4-k)-}$, and nonprotonated species are combined; either term is naturally associated with either extreme of acidification (0 and > 2.5 equiv of acid). These are multiplied by fractions that take into account the amount of light absorbed by each species; the absorbed light depends on the concentration of the particular species divided by the total concentration of decatungstate.²⁹ For generality, steady-state terms include the total alkane quenching rate constant, k_{qk} , instead of k_l .³⁰ The factor α inserted in front of the fractions take into account the thermal reduction of decatungstate by alkyl radical intermediates. α is dependent on the concentration of added acid. It is equal to 1 when there is no acid present and the thermal reduction of decatungstate by radicals is negligible. It tends toward 2 above a certain low threshold concentration of $H_kP^{(4-k)-}$, where alkyl radicals generated from P^{4-} can be oxidized by $H_kP^{(4-k)-}$, leading toward a doubling in the reduction rate. In the biphasic region, $\alpha \approx 2$ at early times and decreases toward 1 as the concentration of $H_kP^{(4-k)-}$ is depleted. For cyclooctane and *cis*-1,2-dimethylcyclohexane, the approximately linear increase in quantum yields and corresponding changes in the product distributions predicted by this equation are experimentally observed between 1 and 2.5 equiv of added acid and between 0 and 2.5 equiv of added acid, respectively.

As a consequence of the thermal radical oxidation component, which causes an apparent increase in the rate of ~ 2 , the photooxidation of alkanes in acidified media with $\phi_{max} \approx 1$ correlates with a "true" quantum yield of 0.5 for reaction of the excited state. Thus, the constant $f_k k_k / k_{qk} = 0.5$ in the steady-state term at high cyclooctane concentrations; f_k , k_k / k_{qk} , or both are smaller than unity.³¹ The quantum yield enhancement resulting from acidification can result if f_l , k_l / k_{qk} , or both increase. The value of

(29) Since the absorption envelopes of both forms of decatungstate have similar shapes and extinction coefficients, the fraction of incident light absorbed by the protonated species will be given by $([H_kP^{(4-k)-}] / [P^{4-}]_0) I_{aT}$ and that by the nonprotonated species by $([P^{4-}]_0 - [H_kP^{(4-k)-}] / [P^{4-}]_0) I_{aT}$. I_{aT} , defined for eq 17, is to be distinguished from I_{aT} , $I_{aT} = I_{al}$ if only one decatungstate species exists in solution; otherwise $I_{aT} > I_{al}$.

(30) The treatment of quantum yield data is covered in Turro, N. J. *Modern Molecular Photochemistry*; Benjamin/Cummings: Menlo Park, CA, 1978; pp 250–251.

(31) Limiting quantum yields for the photooxidation of organic substrates much smaller than unity have been obtained for other polyoxometalates. One example is in Dimotikali, D.; Papaconstantinou, E. *Inorg. Chim. Acta.* **1984**, *87*, 177.

(28) The lifetime of the weakly emissive excited state of $W_{10}O_{32}^{4-*}$ in solution generated upon excitation by a frequency-tripled YAG laser system (355 nm) has been measured in two different laboratories to be approximately 21 ps (Kozik, M.; Winkler, J.; Hilinski, E. F.; Tate, K.; Duncan, D.; Hill, C. L. Unpublished work). However, the only extensively used solvents that are compatible with all the photochemistry here, water and acetonitrile, quench the excited state.

f_i , which indicates the percentage of active excited states produced, appears not to increase upon acidification since the limiting quantum yields of photoreduction are similar (~ 1) with and without acid for a variety of reactive organic substrates such as benzyl alcohol, tetrahydrofuran, and 2-butanol. An increase in the ratio k_i/k_{qt} thus probably leads to the quantum yield enhancement; this can occur if the redox potential of the excited state increases as discussed in this report.

At the two extremes of acidification, i.e., 0 or > 2.5 equiv of acid, eq 17 reduces to a one-term expression. After removing the light intensity terms and taking reciprocals, one obtains eq 18 for either of the two extremes, which allows quantification of the rate

$$\frac{1}{\phi} = \frac{1}{f_i} \left(\frac{k_{qt}}{k_i} + \frac{k_{dt}}{k_i[\text{RH}]} \right) \quad (18)$$

constants in eq 17. Plots of ϕ^{-1} vs $[\text{RH}]^{-1}$ have been made in acidified (Figure 12) and nonacidified cyclooctane systems. With the f_i set equal to k , the y -intercepts, i , provide $k_{qt}/k_k = 0.86$ for the acidified and $k_{q0}/k_0 = 3.4$ for the nonacidified system. With this same assumption, the slopes, m , give $k_{dk}/k_k = 0.095 \text{ M}$ for the acidified and $k_{d0}/k_0 = 1.63 \text{ M}$ for the nonacidified system. Without approximating the f_i , we obtain $i/m = k_{qt}/k_{dt} = 9.0$ and 2.1 M^{-1} for the acidified and nonacidified systems, respectively. Note from the plot of the acidified system that $1/i = 1/0.86 = 1.16$, approximately equal to the value of 0.98 obtained for the limiting quantum yield at high concentrations of cyclooctane.

Other Lines of Evidence. Further experiments revealing the role of the protons in these phenomena were pursued. The presence of a few equivalents of strong acid catalyzes the isomerization of 2,3-dimethyl-1-butene in acetonitrile solvent in the absence of decatungstate to a distribution consisting mainly of the tetra-substituted alkene.³² This transformation occurs at a rate that can be conveniently measured over a minute-to-hour time scale at room temperature and is not catalyzed by nonacidified decatungstate. The isomerization rate as a function of added decatungstate was analyzed (Figure 12S in the supplementary material). Acetonitrile solutions of triflic acid (2.0 mM) and 2,3-dimethyl-1-butene containing **1** at various concentrations resulted in faster isomerization rates at low concentrations of **1**. At high concentrations of **1**, the isomerization was completely suppressed.

Protons, derived from the alkane substrate, are also generated in the photoreactions, as discussed above. To note if any alkene isomerization resulted from these protons, about 1 equiv of both 1,6-dimethylcyclohexene and 2,3-dimethyl-1-pentene were added to maximally photoreduced systems initially containing $[\mathbf{1}] = 3.2 \text{ mM}$ and cyclooctane substrate in acetonitrile solvent. The isomerization rates were negligible in comparison to those obtained with strong acids such as triflic under similar conditions.

The kinetic data obtained for the nonacidified systems would show a rate increase as a function of irradiation time if all the protons generated from the alkane oxidation did not protonate the photochemically inactive reduced species but rather remained in solution free to protonate the photochemically active $\text{W}_{10}\text{O}_{32}^{4-}$ species, i.e., increase the value of l . Such a rate increase due to the generation of protons in situ, however, is not experimentally observed throughout the course of the reaction. The rates are found to depend on the quantity of light absorbed; the quantum yields remain constant.

Polyoxometalate–Semiconductor Metal Oxide Analogy. Given both the similarities and the fewer number of dissimilarities in the structural, electronic, and macroscopic photochemical properties of polyoxometalates, such as $\text{W}_{10}\text{O}_{32}^{4-}$, versus those of semiconductor metal oxides, such as WO_3 , the studies presented in this paper suggest that protonation of surface oxygen atoms in semiconductors should have particular defensible consequences. One thermodynamic consequence of protonation was indicated

prior to this work, and the data here substantiate this point: A major effect of protonation is an increase in the potentials of both the ensemble of bonding orbitals (valence band in the semiconductors) and the ensemble of antibonding orbitals (conduction band in the semiconductors). The HOMO–LUMO gap (band gap in the semiconductors) is less significantly perturbed in either polyoxometalates or semiconductors upon protonation. Next, protonation of semiconductor surface oxygen atoms should demonstrably increase the kinetic as well as the thermodynamic reactivity of the excited state, to some extent, regardless of the degree of delocalization of the excited state. Delocalization is hard to assess either in polyoxometalates or semiconductor metal oxides, but on the time domains of the oxidations (picoseconds with $\text{W}_{10}\text{O}_{32}^{4-}$)²⁷ a considerable degree of localization may exist in the excited states of both types of materials. Further, protonation of semiconductor surface oxygens should directly impact on the selectivities manifested in their photoredox reactions, particularly those involving organic substrates, by directly affecting the rate of electron-transfer oxidation of organic radical intermediates. Unfortunately the latter area is hard to assess directly, as the literature on semiconductor metal oxide based photooxidations of organic materials involves nearly exclusively reactions conducted under aerobic conditions,² where processes associated with O_2 itself, including the radical chain autoxidation processes, obscure the inherent selectivities associated with attack of the excited metal oxide species on the substrate. A corollary of the above points is that the quantum yields of photoredox, and in some cases photocatalytic, phenomena facilitated by semiconductor metal oxides under anaerobic conditions, may be appreciably higher in the presence of acids that are sufficiently strong to protonate the surface. Inasmuch as surface protonation of semiconductors by addition of strong acids can be effected without decomposition of the oxide in many cases, there are several possibilities for anaerobic organic photochemical transformations that warrant experimental examination. Finally, this work clarifies that protonation of the polyoxometalate $\text{W}_{10}\text{O}_{32}^{4-}$ slows the rate of reoxidation of the reduced forms whether the reoxidation process is reduction of protons to produce H_2 , the predominant process under anaerobic conditions, or reduction of O_2 to produce water. The overall turnover rate is usually affected by protonation as reoxidation of the reduced forms of the photocatalyst is usually rate determining. Qualitatively if not quantitatively similar affects of protonation on the turnover rates in the analogous semiconductor metal oxide photoredox reactions should also be operable. It is clear that careful control of catalyst protonation in both polyoxometalate and semiconductor-based photochemical reactions should lead in many cases to altered selectivities and improved performance.

Conclusions

Eight independent lines of experimental evidence corroborate most of the processes previously demonstrated for the mechanism of photooxidation of alkanes by polyoxotungstates, eqs 2–11,⁵ and establish that protonation of the reactant (oxidized) and product (reduced) forms of **1** takes place in the presence of strong acids. Protonation increases the ground- and excited-state redox potentials of **1** in aprotic media both by $\sim 1 \text{ V}$, while the HOMO–LUMO gap is minimally perturbed. Consistent with this, protonation of **1** results in increases in (1) the rate of eq 4, (2) the quantum yields for alkane photooxidation (by factors up to 25-fold), (3) the ratio of excited-state deactivation by photoredox processes versus radiationless decay, and (4) the rate of thermal radical oxidation by **1**, which has predictable and previously demonstrated consequences on the alkane-derived products. Also consistent with the impact of protonation on redox potentials, the rate of reduced polyoxometalate reoxidation either by H_2 evolution, eq 11, or by O_2 oxidation is 1 order of magnitude slower for the protonated than the unprotonated reduced complex. As the reoxidation processes are rate determining in the overall catalysis, catalytic turnover is slower in the presence of acid.

The data from all these investigations define further the potential and applications of this chemistry and provide some insight

(32) The distribution of alkenes given here resulting from the acid-catalyzed isomerization may not be the one dictated by thermodynamics since side reactions that deplete some alkenes preferentially are indicated. These include hydration and cationic polymerization.

into the effect of surface oxygen protonation on the photodynamic processes of semiconductor metal oxides. All the data reveal that the electronic and structural perturbations of the polyoxometalate complex induced by solvent, including the presence or absence of electron donor–acceptor interactions, salt effects, ion pairing effects, and other medium effects are substantially less important on the photoredox chemistry than those induced by protonation.

Acknowledgment. We thank the National Science Foundation (Grant CHE-9022317) for support of this work.

Supplementary Material Available: Twelve figures addressing kinetics, quantum yield, electrochemical, and spectral (^{183}W NMR and UV–visible) measurements (13 pages). Ordering information is given on any current masthead page.

Polyene 2^1A_g and 1^1B_u States and the Photochemistry of Previtamin D_3

William G. Dauben,^{*,†} Bimsara Disanyaka,[†] Dirk J. H. Funhoff,^{†,‡} Bryan E. Kohler,^{*,§} David E. Schilke,[§] and Boli Zhou[†]

Contribution from the Departments of Chemistry, University of California, Berkeley, California 94720, and University of California, Riverside, California 92521-0403. Received March 7, 1991. Revised Manuscript Received June 11, 1991

Abstract: The quantum yields of the photoproducts from previtamin D_3 were measured at different wavelengths with monochromatic irradiation. While the quantum yield for the cis–trans isomerization decreases with increasing wavelength near 303 nm, the ones for formation of the ring-closure products increase dramatically. This increase in photocyclization yield with decreasing photon energy is attributed to the involvement of both the $1B$ and $2A$ excited states of previtamin D_3 . This hypothesis is supported by measurements of the previtamin D_3 fluorescence spectrum, fluorescence lifetime, wavelength dependence of the fluorescence quantum yield, and temperature dependence of fluorescence intensity. All of these data are integrated into a potential energy surface diagram that is consistent with both the photochemical and spectroscopic behavior.

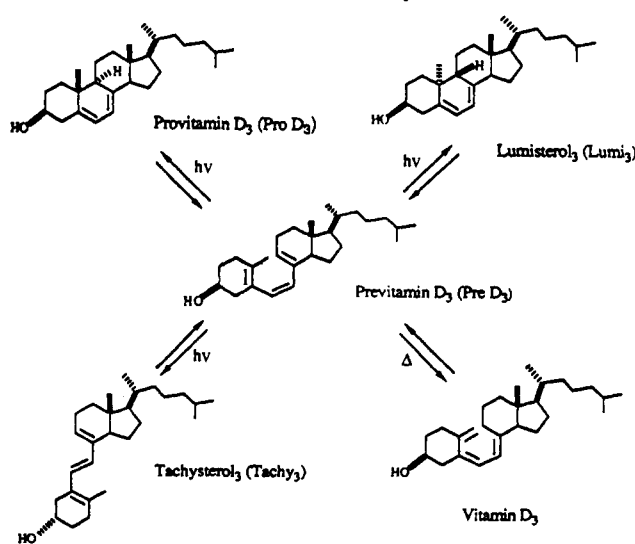
1. Introduction

The photochemistry of previtamin D_3 (pre D_3) has been intensively studied over the last three decades. This has resulted in the identification of the photochemical products and the description of the overall photochemistry (Scheme I).¹ In recent years, the dependence of the observed solution photochemistry on excitation wavelength has been investigated. Because of its importance in optimizing the commercial production of vitamin D_3 via pre D_3 , the photochemical conversion of provitamin D_3 (pro D_3) to pre D_3 has received special attention. It has been found that pre D_3 is formed from pro D_3 in significantly different yields at different excitation wavelengths.²

Later studies have shown that the wavelength-dependent production of pre D_3 comes from an intrinsic wavelength dependence in the photoreactions of pre D_3 .^{3–5} Having determined the quantum yields for photoproducts from pre D_3 at two different irradiation wavelengths (isolated by filter solutions) and found them to be significantly different.³ During the following year, the effect of varying irradiation wavelength was examined at Berkeley with pulsed laser excitation to achieve greater wavelength resolution.⁴ In these studies, quantum yields were most often calculated from photostationary concentrations. Effort was also made to extract quantum yields from the concentration versus time profiles of each component of the system.⁵

A wavelength effect in solution photochemistry can be attributed to a number of ground-state factors: secondary photoreactions by primary photoproducts, selective excitation of thermally equilibrated ground-state conformers, and excitation of ground-state complexes. However, wavelength dependence may also result from excited-state phenomena if photoreaction or other decay channels are competitive with the realization of a thermally equilibrated excited state.⁶ We believe that this is the situation for pre D_3 .

Scheme I. Photoreactions of Previtamin D_3



In an earlier study at Berkeley,⁴ the calculated quantum yields for the formation of pro D_3 and lumisterol $_3$ (lumi $_3$) from pre D_3

(1) General reviews of the photochemistry related to the previtamin D_3 system: (a) Dauben, W. G.; McInnis, D. M. In *Rearrangements in Ground and Excited States*; de Mayo, P., Ed.; Academic Press: New York, 1980; Vol. 3, p 81. (b) Jacobs, H. J. C.; Havinga, E. In *Advances in Photochemistry*; Pitts, J. N., Jr., Hammond, G. S., Gollnick, K., Eds.; Interscience Publishers: New York, 1979; Vol. 11, p 305. (c) Norman, A. W. *Vitamin D*; Academic Press: New York, 1979.

(2) (a) Dauben, W. G.; Phillips, R. B. *J. Am. Chem. Soc.* **1982**, *104*, 355. (b) Kobayashi, T.; Yasumura, M. *J. Nutr. Sci. Vitaminol.* **1973**, *19*, 123. (c) Sato, T.; Yamachuchi, H.; Ogata, Y.; Kunii, T.; Kagei, K.; Katsui, G.; Toyoshima, S.; Yasumura, M.; Kobayashi, T. *J. Nutr. Sci. Vitaminol.* **1980**, *26*, 545. (d) Barton, D. H. R.; Hesse, R. H.; Pechet, M. M.; Rizzardo, E. *J. Am. Chem. Soc.* **1973**, *95*, 2748. (e) Pfoertner, K.; Weber, J. P. *Helv. Chim. Acta* **1972**, *55*, 921. (f) Pfoertner, K. *Helv. Chim. Acta* **1972**, *55*, 937.

[†]University of California, Berkeley.

[‡]Recipient of a Feodor–Lynen Fellowship of the Alexander von Humboldt Foundation, 1986–1987.

[§]University of California, Riverside.